UNIVERSITÉ DE GENÈVE
FACULTÉ DES SCIENCES DE LA SOCIÉTÉ

UNIVERSITÉ DE GENÈVE
INSTITUT DES SCIENCES DE L'ENVIRONNEMENT

UNIVERSITÉ DE GENÈVE
FACULTÉ DES SCIENCES

COMPLEMENTARY CERTIFICATE IN GEOMATICS

A comparison of the Plant Phenology Index (PPI) and the Normalized Difference Vegetation Index (NDVI) in mountainous area

Certificate thesis

Candidate: Dimitri Charrière

Thesis supervisor: Dr. Gregory Giuliani

January 2024

Abstract

Cold ecosystems are experiencing a warming rate that is twice as fast as the global average and are particularly vulnerable to the consequences of climate change. Solid monitoring process are required to understand the response of ecosystems to these abrupt changes. The Normalized Difference Vegetation Index (NDVI) is one of the most widely used remote sensing index for vegetation monitoring. However, it suffers from limitations in retrieving consistent signal for areas covered by seasonal snow and for coniferous forest. The Plant Phenology Index (PPI) has been developed to overcome these issues, primarily in northern latitudes. It could be used in other biome but has not yet been specifically assessed in mountainous areas despite similar climatic conditions. The aim of this study is to contribute to the development of remote sensing monitoring for vegetation by conducting a comparison and an assessment of the PPI and NDVI in mountainous regions. We focus our study on the canton of Valais (CH) in the European Alps and also use eddy covariance derived Gross Primary Production (GPP) from Torgnon (IT) for ground data correlation analysis. We use data derived from the MultiSpectral Instrument on the Sentinel-2 satellite constellation for the year 2018-2022 to construct time series for four types of vegetation: deciduous trees, coniferous trees, grasslands and shrubs. Regarding seasonal cycle, the NDVI is particularly noisy at the beginning/end of the snowed season and for coniferous trees, which is consistent with its known snow sensitivity issue and difficulties to retrieve signal variation in dense and evergreen vegetation. The PPI seems to deal with these problems but tends to overestimate peak values, which could be attributed to its logarithmic formula and derived high sensitivity to variations in near-infrared (NIR) and red reflectance variations during peak growing season. Concerning seasonal parameters retrieval, we find consistent results for the start of the season (SOS) and end of the season (EOS) between indices, except for coniferous trees. Peak of the season (POS) results exhibit important differences between the indices. Correlation analysis with ground-measured GPP in an alpine grassland in Torgnon (IT) shows a high Spearman correlation coefficient for both NDVI (0.75) and PPI (0.72). Our findings are coherent with the existing literature and contribute to the development of more accurate remote sensing vegetation monitoring. The PPI is a robust remote sensed index for vegetation monitoring in seasonal snow-covered and complex mountain environments.

Summary

List of abbreviations

CLMS:	Copernicus land monitoring service
DOY:	Day of the year
DVI:	Difference vegetation index
EO:	Earth observation
EOS:	End of the season
EVI2:	Two-band enhanced vegetation index
FAPAR :	Fraction of absorbed photosynthetically active radiation
HR-VPP:	High-resolution vegetation phenology and productivity
GEE:	Google earth engine
GPP:	Gross primary production
GCC:	Green chromatic coordinate
ICOS:	Integrated carbon observation system
LAI:	Leaf area index
MODIS:	Moderate resolution imaging spectroradiometer
NARI:	Normalized anthocyanin reflectance index
NCRI:	Normalized chlorophyll reflectance index
NDVI:	Normalized difference vegetation index
NIR:	Near-infrared
POS:	Peak of the season
PPI:	Plant phenology index
QFLAG2:	Quality flag
SOS:	Start of the season
ST:	Seasonal trajectory
VI:	Vegetation index

List of figures

List of tables

1. Introduction

1.1. Context

Cold ecosystems, i.e. arctic and alpine regions, are suffering a warming rate twice higher than the global average and are particularly exposed to climate change consequences (Beniston et al., 2018; Gobiet et al., 2014; IPCC, 2021). Temperature (Berner et al., 2020; Corona-Lozada et al., 2019; Francon et al., 2017; Körner, 2021) and snow cover expansion and duration (Choler, 2015; Körner, 2021; Wipf et al., 2009) are known as major limiting factors for vegetation growth in these environments and both are influenced by climate change.

In the Alps, the vegetation executes its seasonal phenological cycle during the snow-free period (Vorkauf et al., 2021). As mentioned by Leuschner & Ellenberg (2017), length of the growing period is one of the main determining factors of productivity. Therefore, vegetation dynamics are influenced by climate change which induce several consequences in the Alps, such as phenology and productivity shifting and vegetation greening (Asam et al., 2018; Choler et al., 2021; Francon et al., 2017, 2020; Tang et al., 2016). However, these links remain poorly understood and require extensive monitoring in space and time.

Remote sensing and derived vegetation indices offer the opportunity to observe vegetation dynamics over wide areas and temporalities (Corona-Lozada et al., 2019; Smets et al., 2022; Xie et al., 2008). Recently launched high spatial and temporal resolution optical sensors (e.g., MultiSpectral Instrument on board Sentinel-2) provide new possibilities for more detailed ecosystems monitoring, such as mountain vegetation dynamics (Smets et al., 2022).

The Normalized Difference Vegetation Index (NDVI) is one of the most widely used vegetation index in the past decades (Carlson, 2016; Choler et al., 2021; Jin & Eklundh, 2014; Tian et al., 2021; Tucker, 1979; Xie et al., 2008). However, it suffers from limits for vegetation state retrieving, notably for seasonal snowed environments and coniferous forest (Jönsson et al., 2010). The Plant Phenology Index (PPI) has been developed recently to overcome these limitations and improve plant phenology monitoring, notably in Arctic areas, and showed great performance (Jin et al., 2017; Jin & Eklundh, 2014). Since, some studies provided new insights for vegetation monitoring with PPI in arid ecosystems (Abdi et al., 2019) and across Europe (Tian et al., 2021). To our knowledge, the PPI performance has not been assessed specifically for complex mountainous environment.

This study seeks therefore to provide new perspectives to retrieve vegetation dynamics in mountain areas. As Arctic environment, mountain areas and more specifically the European Alps are facing a seasonality marked by the presence of snow and low temperatures. Therefore, the PPI could provide new insights for coping with the limitations of NDVI and enhance the monitoring of vegetation in complex environments such as mountain areas.

To do so, we will compare and assess the capacity of PPI and NDVI to retrieve dynamics of four vegetations types: deciduous trees; coniferous trees; grasslands; shrubs. Our area of interest is the canton of Valais (CH) straddling the Bernese and Pennine Alps. In a first step, we will elaborate a vegetation cover map of these four vegetation types. In a second step we will construct and compare Sentinel-2 derived time series of PPI and NDVI and extract seasonal parameters (i.e., start of the season, end of the season and peak of the season). In a final step, we will compare their performance to retrieve ground derived Gross Primary Production (GPP) on the alpine site of Torgnon (IT).

1.2. Theoretical background

1.2.1. Vegetation phenology and dynamics in the Alps

Vegetation or plant phenology could be described as "the study of recurring events in the life cycle of plants" (Tang et al., 2016, p.1). As exposed by Tang et al. (2016), phenological shifts are phenomenon that can be seen as an indicator of the climate change ecological impacts. Furthermore, the consequences of phenological stages shifting (e.g. start, duration, end of the season) are multiple on the ecosystems such as leaf area, carbon cycle or species distribution. However, there is an incomplete understanding of the mechanistic links between climate change and these shifts.

In addition, a global vegetation greening trend has been identified since the 1980s (Filippa et al., 2019; Keenan & Riley, 2018). In the cold areas, the greening is consistent with the recent temperature increase (Keenan & Riley, 2018). While this trend is well-documented in the Arctic (Berner et al., 2020; Myers-Smith et al., 2020), there are only few studies in the European Alps (Carlson et al., 2017; Choler et al., 2021). Therefore, the recent technological advancements, in particular remote sensing, offer new possibilities for vegetation dynamics monitoring, particularly in wide and complex ecosystems (Smets et al., 2022; Tang et al., 2016).

1.2.2. Remote sensing for vegetation monitoring

As described by Xie et al. (2008), a remote sensing sensor is a tool that collects data (e.g. spectral) about an object or a scene from a distance. Objects (including vegetation) possess their own spectral signature. It is therefore possible to characterize the type and condition of vegetation from its spectral characteristics. The fraction of photosynthetically active radiation could be retrieved using the radiance in the red and near-infrared (NIR) spectrum, with potential addition of other wavelengths. Therefore, spectral band of these wavelengths of interest are included in the construction of vegetation indices (VIs) like NDVI and PPI (Jin & Eklundh, 2014; Tucker, 1979; Xie et al., 2008).

Different sensors have different spectral, spatial and/or temporal characteristics and are therefore more or less adapted according to the target (Xie et al., 2008). For global, continental to national mapping, the MODerate resolution Imaging Spectroradiometer (MODIS) is extensively used (e.g., Choler et al., 2021; Jönsson et al., 2010; Stanimirova et al., 2019), due to its 1 to 2 days temporal resolution and 250 to 1000 m spatial resolution (depending on the spectral band). Landsat 8/9 satellites are widely used for regional scale with a spatial resolution of 30 m and a temporal resolution of 16 days (e.g., Carlson et al., 2017; Poussin et al., 2021). More recently Sentinel-2 satellites constellation and their multispectral products offer new observation possibilities for continental to local mapping with a spatial resolution of 10 m and a revisit time of 5 days (Tian et al., 2021).

Land use and land cover changes are of primary importance for many domains in science and practical applications (Giuliani et al., 2022). Regarding vegetation, the red-edge band of the multispectral sensor on board Sentinel-2 offers new mapping possibilities, e.g. for grasslands and shrubs, in addition of the increased spatial resolution (Bayle et al., 2019; Filippa et al., 2022).

By studying phenological aspects, seasonal trajectories and phenological metrics could be retrieved from satellite imagery. It therefore permits phenological monitoring through intra- and inter- annual time steps at different spatial scale, depending on the study goal (Smets et al., 2022).

Concerning technical and practical aspects of Earth Observation (EO) data, as Giuliani et al. (2017) noted, an increasing proportion of them are freely and openly available. Although it's a great opportunity for data access, the important volume of these ones needs to be treated and integrated in an appropriate way by the user, which is a known issue. To overcome this problem, recently

constructed data cubes provide structured and ready to-use data as a multi-dimensional array (Baumann, 2017; Giuliani et al., 2017). Therefore, parameters for environmental monitoring (e.g. vegetation) could be directly implemented in a data cube and released as analysis ready data (Giuliani et al., 2017).

1.2.3. Vegetation indices

NDVI

As mentioned before, the NDVI is one of the most widely used index for vegetation studies and monitoring. As noted by Jin & Eklundh (2014), the popularity of this index is due to its relative robustness against noise and sun-sensor geometry variations and the availability of long-term time series at a global scale. The NDVI is calculated such as :

$$NDVI = \frac{\rho\,\mathrm{NIR} - \rho\,\mathrm{Red}}{\rho\,\mathrm{NIR} + \rho\,\mathrm{Red}}$$

where ρ NIR is reflectance in the near infrared band and ρ Red is reflectance of the red band. The result is used as a proxy of the land surface greenness (Choler et al., 2021; Tucker, 1979) : a value of - 1 indicates a water surface ; a value between 0 and 0.2 corresponds to almost non-vegetation areas; a value close to 1 signifies a dense and green vegetation cover. A healthy vegetation cover tends to have a high absorption of photosynthetically active radiation, captured in the red band and a low absorption of low infrared radiation, which could induce damage to plants due to overheating (Carlson, 2016). This index however suffers from two major limitations (Jin & Eklundh, 2014) : (i) its sensitivity to soil background (e.g., snow) and (ii) its saturation at high vegetation density. Particularly, this index express difficulties to catch small amplitude variation, like evergreen coniferous forest (Tian et al., 2021).

PPI

Jin & Eklundh (2014) have developed a physically-based spectral index to characterize the phenological dynamics of vegetation: the Plant Phenology Index (PPI). This index has an almost linear relationship with the green Leaf Area Index (LAI) and reposes on the NIR and Red reflectance values. It is based on Beer's law, modified for canopy reflectance. PPI has the same unit as LAI ($m^2 \cdot m^{-2}$) and is formulated as (Jin et al., 2017; Jin & Eklundh, 2014; Tian et al., 2021) :

$$PPI = -K \times \ln\left(\frac{DVI_{max} - DVI}{DVI_{max} - DVI_s}\right)$$

where *DVI* (Difference Vegetation Index) is the difference between NIR and Red reflectance; *DVImax* is the maximum canopy *DVI* of a specific site; *DVIs* is the soil *DVI*. *K* is a gain factor given by:

$$K = \frac{1}{4 \cdot (dc + 0.5 \cdot (1 - dc)/cos(\theta_s))} \times \frac{1 + DVI_{max}}{1 - DVI_{max}}$$

where *dc* is an instantaneous diffuse fraction of solar radiation, when the sun is at zenith angle θ_s (obtained from the corresponding scene metadata), calculated as:

$$dc = 0.0336 + 0.0477/cos(\theta_s)$$

For further information about the PPI formulation, we refer to the reference paper of Jin & Eklundh (2014).

The PPI is relatively insensitive to snow cover in comparison to NDVI. Furthermore, PPI is strongly correlated with GPP (i.e. the amount of carbon biomass produced by vegetation for a given length of time) and could therefore complement or substitute NDVI for vegetation growth dynamics monitoring, particularly for evergreen coniferous forest with relatively low seasonal amplitude (Jin et al., 2017, 2019; Jin & Eklundh, 2014; Tian et al., 2021). As mentioned by Tian et al. (2021), PPI has been primary tested in boreal areas using MODIS data despite its potential for phenology mapping through different ecosystems at higher resolution. Therefore, they call for more PPI performance testing across different biomes with more accurate resolution. In their study, they calibrated vegetation phenology Sentinel-2 dataset with ground data of GPP (derived from eddy covariance Fluxtower), Phenocam green chromatic coordinate (GCC) and phenology ground observations from the Pan-European Phenological database (PEP725) network. To do so, they compared the performance of NDVI, the two-band enhanced vegetation index (EVI2) and PPI for Europe-wide seasonal phenology mapping and phenology metrics retrieval. The PPI showed promising results by performing better for GPP photosynthetic phenology mapping and for retrieving phenological phases issued form PEP725 data. However, no conclusive results have been drawn from greenness phenology, retrieved form Phenocam GCC data. In another way, Abdi et al. (2019) used the PPI to build a remote sensed GPP estimation model for semi-arid ecosystems of Africa. PPI-based GPP model demonstrated superior performance compared to three others commonly used remote sensing models. The PPI has been recently implemented in the European Union's Earth Observation Programme (Smets et al., 2022).

1.2.4. Copernicus High-Resolution Vegetation Phenology and Productivity (HR-VPP) product

The European Union's Earth Observation Programme is named Copernicus (https://www.copernicus.eu). Following Smets et al. (2022), the program provides freely and openly information based on satellite Earth observation about six thematic: (i) atmosphere, (ii) marine environment, (iii) land, (iv) climate change, (v) emergency management and (vi) security. Information about vegetation are supplied by the Copernicus Land Monitoring Service (CLMS, https://land.copernicus.eu/) and are derived from the Sentinel-2 satellites constellation (2A and 2B). Therefore, data user benefit from the high resolution and revisit time from the latter, respectively 10 m and 5 days, grouped under the High-Resolution Vegetation Phenology and Productivity (HR-VPP) product suite. It comprises three product packages:

1. The raw Vegetation Indices (VIs): in addition of the PPI and NDVI, the LAI and the Fraction of Absorbed Photosynthetically Active Radiation (FAPAR) are provided for every Sentinel-2 observation.
2. The Seasonal Trajectories (STs): these products are based on the raw PPI observations. A smoothing and gap filling function is applied on a seasonal basis to produce a regular time series. A derived image every 10 days is finally provided.
3. The Vegetation Phenology Parameters (VPPs) : derived from the STs of PPI, these products provide phenology metrics (e.g., start, peak, end of the season).

1.2.5. Time series analysis

Following Kuenzer et al. (2015), time series correspond to real-value, continuous or discrete series of data, with values referring to equidistant points in time. The temporal variations of values could therefore emphasis periodic, cyclic, transient, or random dynamics. They are helpful in a large scope of disciplines from economics to astronomy or geophysics but also remote sensing. By using satellite images, we could retrieve time series at the revisit time interval. The revisit time is about 16 days for Landsat. This relative long revisit time with the possibility of clouded observation contamination does not offer reliable opportunity for phenology studies (Tian et al., 2021). Therefore, Sentinel-2 and its

5-days revisit time offer a good opportunity. However, the clouded observation contamination risk persists. We therefore need to apply a fitting function to retrieve the vegetation seasonal signal.

As mentioned by Eklund & Jönsson (2017), time series of vegetation index derived from satellite spectral data are useful to follow seasonal vegetation development through a simple season but also through multiple years. Therefore, they developed the TIMESAT software (Jönsson & Eklundh, 2002; 2004). It's a useful software package to analyze time series, particularly of satellite sensor data (Eklund & Jönsson, 2017). It permits to explore time series data in details and retrieve seasonality parameters, such as start of the season, peak of the season or end of the season.

1.2.6. Fluxtower data

FLUXNET is a global network that provides concentration values of carbon dioxide and water vapor in addition of micrometeorological and energy variables which permits to measure flux between the biosphere and the atmosphere (Baldocchi et al., 2001). Flux measurement tower combined with the eddy covariance technique enables a direct and non-destructive calculation of the greenhouse gases and energy exchange between an ecosystem and the atmosphere, usually at a half-hour time step. It permits therefore to : (i) study ecological and physiological development of single ecosystems; (ii) serve as ground measurement for the calibration of models and remote sensing operations (Papale, 2020). The GPP could therefore be estimated using the measured CO_2 fluxes to parameterize a model based on light-response curve and vapor pressure deficit, both of which are key factors for photosynthesis (Pastorello et al., 2020). These data have been used in precedent remote sensing studies for ground validation (e.g., Abdi et al., 2019; Tian et al., 2021).

1.3. Problematic and research questions

The aim of the study is to contribute to the development of remote sensing monitoring for vegetation by comparing and assessing the performance of the Plant Phenology Index (PPI) and Normalized Difference Vegetation Index (NDVI) in mountainous areas. It seeks to provide new insights into remote sensing methodologies for vegetation monitoring in mountainous areas to enhance our understanding of vegetation dynamics in complex environments. Therefore, we look to answer to the following questions:

- How do the Plant Phenology Index (PPI) and the Normalized Difference Vegetation Index (NDVI) retrieve the seasonal cycle of different vegetation types in mountainous areas?
- How do the Plant Phenology Index (PPI) and Normalized Difference Vegetation Index (NDVI) differ (or not) by retrieving seasonality parameters of different vegetation types in mountainous areas?
- How are the Plant Phenology Index (PPI) and the Normalized Difference Vegetation Index (NDVI) correlated with ground-measured Gross Primary Production (GPP) in mountainous areas?

2. Materials and Methods

The successive stages of the methodology are shown in figure 1. We used the R environment (R Core Team, 2023) for images processing and statistical analysis, TIMESAT for time series processing (Jönsson & Eklundh, 2004) and Google Earth Engine (Gorelick et al., 2017) and ArcGIS pro software (Esri Inc., 2023) for vegetation cover mapping.

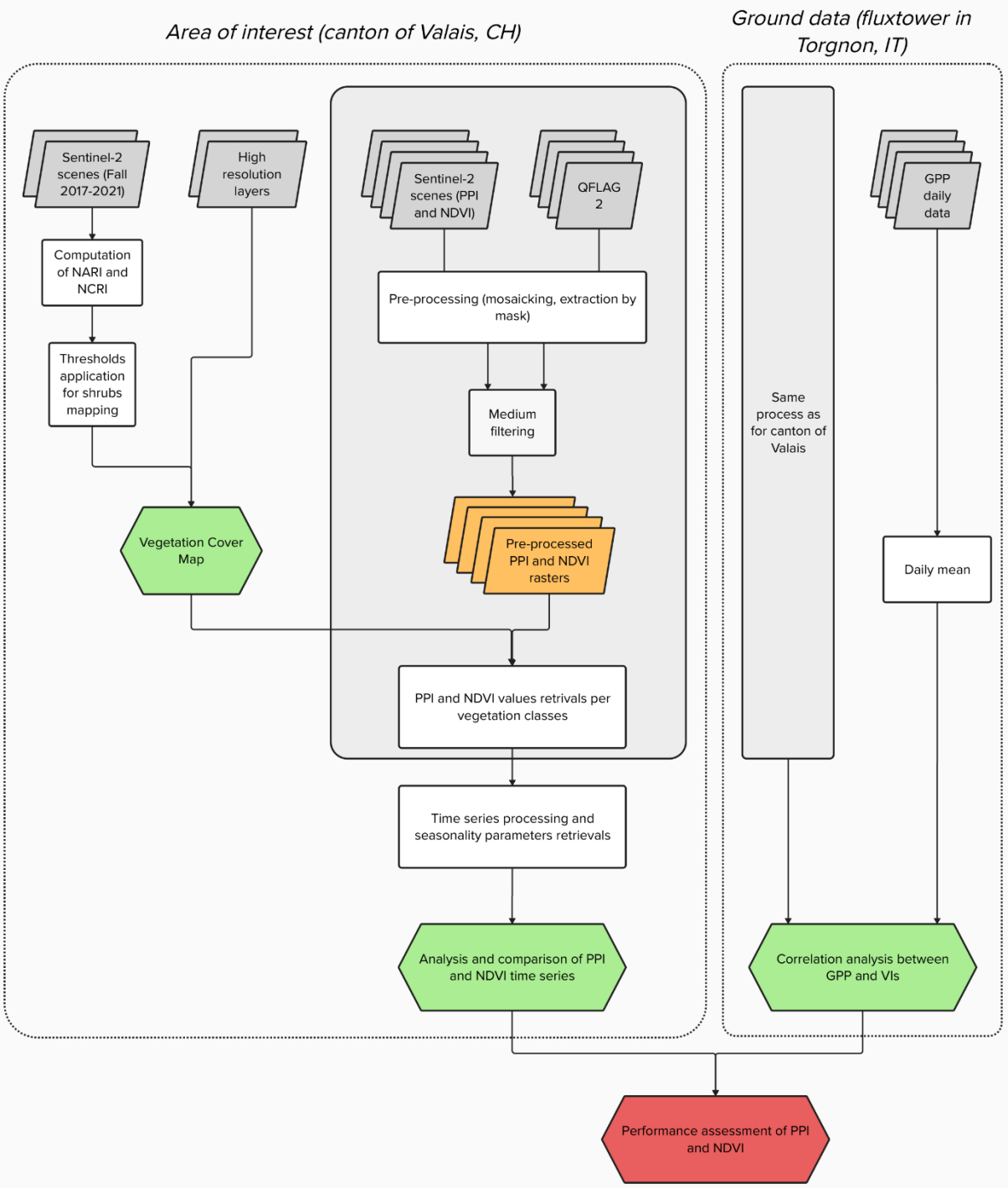

Figure 1 : General workflow

2.1. Study area

The study area is delimited through the borders of the mountainous canton of Valais in Switzerland (figure 2). The lowest point is at 372 m above sea level (a.s.l.) at the Geneva Lake and the highest at 4634 m a.s.l. at the Dufourspitze. The surface of the area of interest is about 5224.35 km^2. The Valais, located in the western European Alps, comprises several valleys, with the Rhône Valley being the primary one. As other mountain regions, the canton is therefore characterized by a high diversity of ecosystems due to its diverse geographical features (Körner, 2021). Since no fluxtower is located in the Valais, we also studied the area near the Torgnon Fluxnet station, located in the Aosta Valley (IT). It's a grassland situated at 2160 m a.s.l.

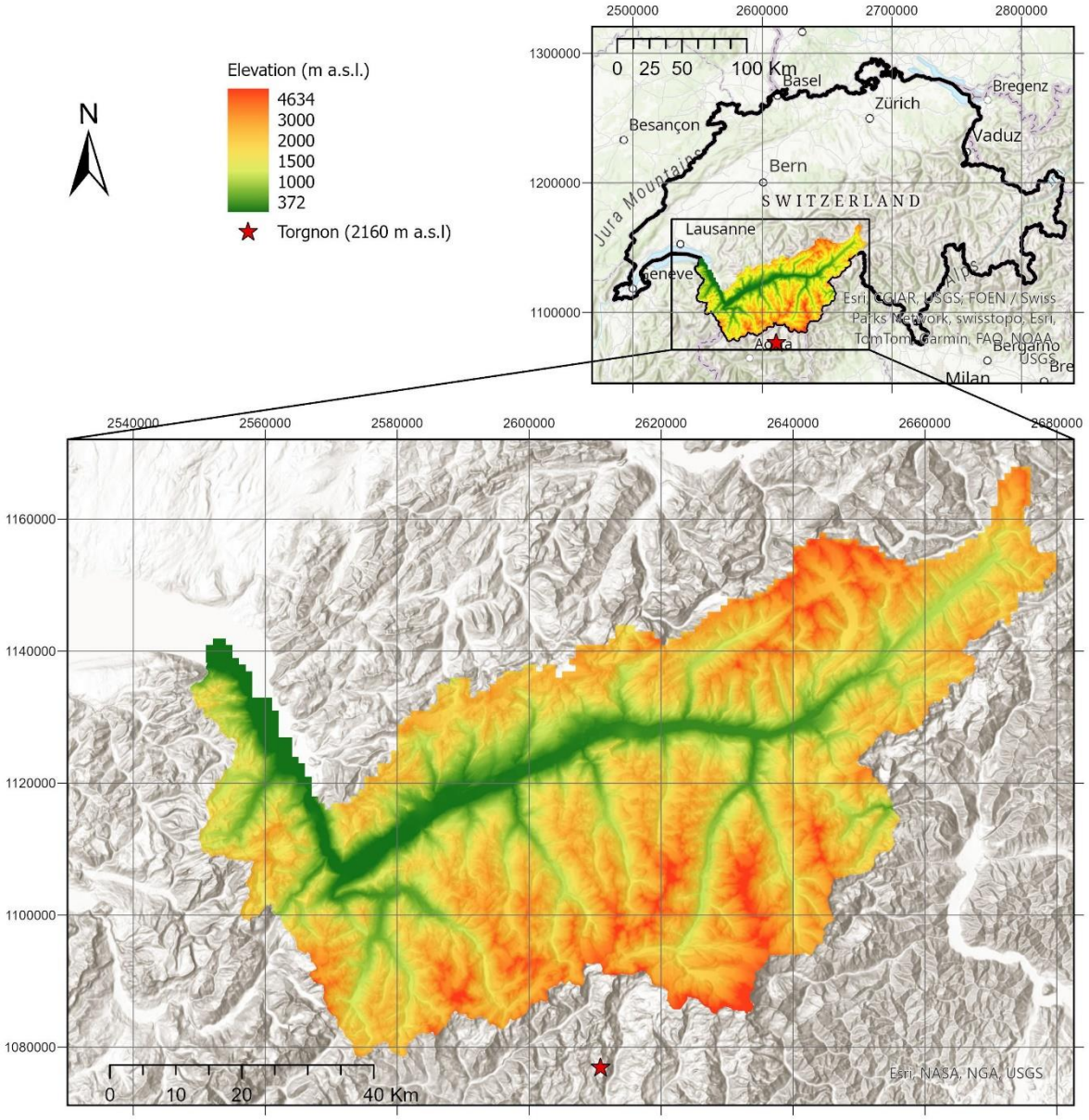

Figure 2 : Localization of the canton of Valais (CH) and Torgnon (IT)

2.2. Satellite Data

Satellite Data have been obtained for: (i) the vegetation cover classification, (ii) the comparison of PPI and NDVI on the Valais territory, (iii) the correlation analysis with the GPP of the Torgnon FLUXNET station.

For the first cited, we used two high resolution layers of the CLMS (European Environment Agency, 2020a, 2020b) : Forest type (2018) and Grassland (2018). These are two raster files with a resolution of 10x10m characterizing broadleaf forest, coniferous forest for the first layer and grasslands for the second layer. For the shrubs mapping, following the methodology proposed by Bayle et al. (in press), we used Google Earth Engine (GEE) to compute the median of the Normalized Anthocyanin Reflectance Index (NARI) and the Normalized Chlorophyll Reflectance Index (NCRI) for each year between 2017 and 2021 for the autumn (September 1st to November 1st) and then computed the median of the five years. The detailed methodology is explained in the section 2.3.

For the second point, we downloaded from the WEkEO platform (https://www.wekeo.eu/) all the PPI and NDVI Sentinel-2 scenes for the years 2018 to 2022 (European Environment Agency, 2021a, 2021b), for the 4 tiles covering the Valais: T32TLS, T32TMS, T32TMR, T32TLR. It corresponds to Sentinel-2A or Sentinel 2-B L1C files, because the L2A data availability on the WEkEO platform was limited (Smets et al., 2022). There are 73 observations per year at 5 days of interval, beginning the 05-01-2018, resulting in 1460 images per index, 2920 in total (> 600 Go). In addition, for each observation date, a quality layer (named QFLAG2) was downloaded. It corresponds to a bitwise encoded status map which indicates if the pixel is water or land, cloud, snow or shadow (Smets et al., 2022).

For the third point, the Torgnon FLUXNET station is located in the area of the T32TLR tile. Therefore, no additional satellite data was necessary.

2.3. Vegetation cover

Regarding the vegetation cover classification, three vegetation classes have been extracted from the High Resolution Layers of the CLMS: deciduous and coniferous trees and grasslands. We used the *terra* package (Hijmans, 2023a) implemented in R to extract the information by the mask of the Valais. The limits of the canton have been obtained from the swissBOUDARIES3D product (Swiss Federal Office of Topography, 2023).

To retrieve the shrubs layer, we followed the methodology proposed by Bayle et al. (in press). To do so, all the available Sentinel-2 scenes for the Valais for the years 2017 to 2021 from the September 1st to the November 1st have been acquired in GEE. In a second step, the Sentinel-2 cloud probability product has been applied on every scene with a threshold of 0.65 to remove the clouds and clouds shadows. Third, the NARI and NCRI have been computed on the all the scenes and a median per year has been extracted. Finaly, we computed a median of the 5 years.

The NARI is sensitive to the plant canopy anthocyanin content. Using this index, Bayle et al. (2019) constructed a methodology to improve the mapping of mountain shrublands. As they noted, shrublands are dominated in the European Alps by *Ericaceae* (i.e., *Vaccinium spp.* and *Rhododendron ferrugineum*). These species have the particularity to accumulate red anthocyanin pigments in the late autumn. This characteristic offers an opportunity to differentiate *Ericaceae* shrublands from other vegetation types. Indeed, as exposed by Bayle et al. (2019), their presence is often underestimated and confounded with grasslands. Therefore, using multi-spectral instrument on board the Sentinel-2 satellites, the accuracy of shrublands mapping could be improved, following this NARI calculation (Bayle et al., 2019) :

$$NARI = \frac{\frac{1}{\rho\ \text{Green}} - \frac{1}{\rho\ \text{Red-edge}}}{\frac{1}{\rho\ \text{Green}} + \frac{1}{\rho\ \text{Red-edge}}}$$

where ρ Green is reflectance in the Green band, ρ Red-edge is reflectance of the Red-edge band.

The NCRI is a normalized adjustment of the canopy chlorophyll content proposed by Bayle et al. (in press). It permits, in addition of the NARI to discriminate forest from *Ericaceae*-shrubs and grasslands (figure 3). NCRI is therefore obtained using the band 5 (Red-edge) and the band 7 (Red-edge 2) from Sentinel-2 and is computed as follow (Bayle et al., in press) :

$$NCRI = \frac{\frac{1}{\rho\ \text{Red-edge}} - \frac{1}{\rho\ \text{Red-edge 2}}}{\frac{1}{\rho\ \text{Red-edge}} + \frac{1}{\rho\ \text{Red-edge 2}}}$$

where ρ is the reflectance in the respective Red-edge or Red-edge 2 band.

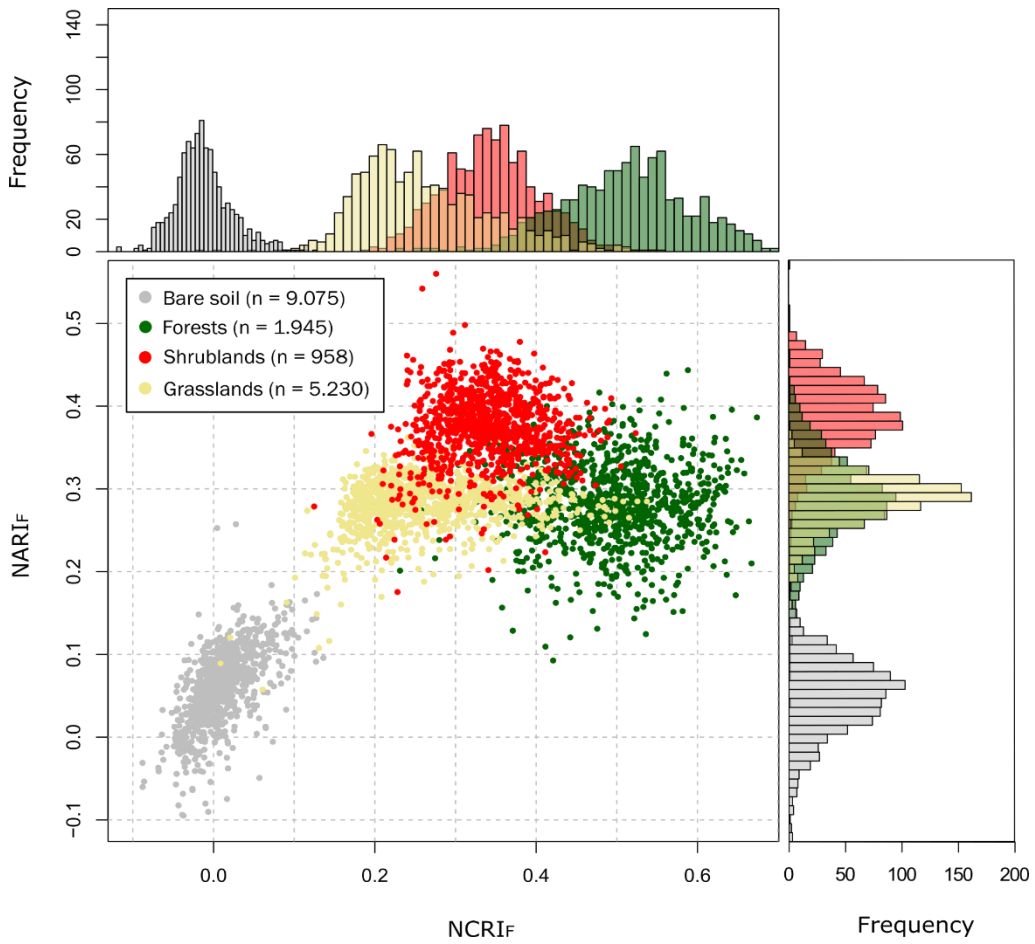

Figure 3 : Resulting distribution of training samples for bare soil, forests, shrublands and grasslands using a discrimination methodology with the combination of NARI and NCRI (Bayle et al., in press)

Following the recommendations of Bayle et al. (in press), we applied a threshold of > 0.325 for the NARI and a threshold of < 0.42 for the NCRI to discriminate the *Ericaceae*-shrublands (see figure 3).

The resulting shrubs layer has a resolution of 20x20 meters. We therefore resampled and reprojected this raster layer using the nearest neighbor method to correspond to the 10x10 m resolution of the Copernicus High Resolution layers. It is important to note that this methodology doesn't permit to identify non-*Ericaceae* evergreen shrubs like *Juniperus* and results in an incomplete mapping of shrublands (Bayle et al., 2019, in press).

The final vegetation cover map was obtained by attributing the corresponding classes to each pixel of the Valais in a single raster layer.

2.4. Vegetation Indices Processing

Concerning the vegetation indices, a common pre-processing workflow has been applied to PPI, NDVI and QFLAG2 images. First, using the *raster* R package (Hijmans, 2023b) implemented in R, one image per index/flag per date has been created by mosaicking the 4 tiles and applying a mean function for the overlying pixels. Second, we extracted the values of the 3 variables by the mask of the Valais. Afterwards, following the recommendation of Smets et al. (2022), we applied a medium filter by masking the overlying PPI and NDVI pixel for the QFLAG2 values 4 to 2048, corresponding to cloud and shadow filtering with the addition of surrounding pixels. Finaly, the PPI and NDVI images have been cropped to our area of interest, i.e. the limits of the canton Valais.

2.5. Retrieval of PPI and NDVI values and Processing of Time series for the Different Vegetation Classes

To retrieve the PPI and NDVI values per vegetation classes and per date, we first resampled the vegetation cover map using the nearest neighbor method to correspond to the 10 m resolution and extension of the cropped PPI and NDVI images. Secondly, we used the zonal function of the *terra* R package (Hijmans, 2023a) to extract the mean PPI and NDVI values per vegetation types for every observation. We saved the results in form of dataframes to mobilize them afterwards in the construction of time series.

To further analyze VIs, we therefore built time series and fitted double logistic functions using the TIMESAT software (Jönsson & Eklundh, 2002; 2004). Based on Eklund & Jönsson (2017) and two other studies using TIMESAT (Karkauskaite et al., 2017; Stanimirova et al., 2019), we first removed the spikes and outliers by attributing a median filtering of 1.5. In a second step, we applied two consistent data ranges for each VI, respectively -1 to 1 for NDVI and 0 to 3 for PPI. Thirdly, since the noise of VI from remotely sensed data is mostly negatively biased, we applied an adaptation to the upper envelope with a strength of 3. It consists of a multi-step process to decrease the weight of low data. Finaly, we selected a season parameter of 1 to fit one season per year. As mentioned by Eklund & Jönsson (2017), the success of the fitting process to the time series is more an art than a science and resides in a visual examination, dependent of the type of noise and disturbances in the data of interest.

2.6. Seasonality parameters retrieval

We also used the TIMESAT software to retrieve seasonal parameters such as start of the season (SOS), peak of the season (POS) and end of the season (EOS). To do so, we applied the method based on the seasonal amplitude (Eklund & Jönsson, 2017). The SOS and EOS occur therefore when the fitted curve has reached a certain fraction of the difference between the base level and the POS. Based on the PPI calibration performed by Tian et al. (2021), we applied respectively thresholds of 0.4 for NDVI and 0.25 for PPI to retrieve the SOS. For the EOS, we used thresholds of 0.5 for NDVI and 0.15 for PPI.

2.7. Ground data

To assess the performance of the PPI and the NDVI on a specific alpine site, we applied the same methodology as Tian et al. (2021) for the GPP/VIs correlation analysis for the FLUXNET station of Torgnon in the Aoste Valley. We therefore retrieve the GPP data for this flux tower and then extracted the VIs for the 2018-2020 period. To do so, we obtained the GPP data from the FLUXNET network via the Integrated Carbon Observation System (ICOS) Data portal (Cremonese et al., 2021). The Torgnon FLUXNET data set provides data from 2008 to 2020. According to the methodology applied by Abdi et al. (2019) and Tian et al. (2021) regarding the ground data sources, we used the daily GPP_DT_CUT_MEAN data set, which is the mean Gross Primary Production using the daytime partitioning method and the Constant USTAR Threshold (see Pastorello et al., 2020, for more detailed information). We therefore extracted daily GPP data from 2018 to 2020. For the VIs, we constructed a buffer of 100 m around the flux tower and then applied the same process as explained in the 2.4. section. We further extracted the PPI and NDVI values for each observation. In a final step, we used the *chart.Correlation* function from the *PerformanceAnalytics* package (Peterson & Carl, 2020) with the Spearman method to conduct the correlation analysis.

3. Results

3.1. Vegetation cover map

The resulting vegetation cover map (figure 4) and the derived surface and altitude metrics (table 1) show specific vegetation patterns for the Valais. Deciduous trees are concentrated in valleys at lower altitude and correspond to a proportion of 9.3 % (i.e., 484 km^2) of the entire Valais surface. Coniferous trees are mainly situated at a higher altitude and cover 13.8 % of the canton territory, which corresponds to 722 km^2. Grasslands are the most widespread vegetation class with a 1176 km^2 surface area, which is equivalent to 22.5 % of the Valais. They are mainly located above the treeline, although they are also present in valleys. Their mean altitude is above 2000 m. Shrubs are the vegetation class with the higher altitude mean (i.e., 2103 m). They also have the smallest surface area with a proportion of 2.5 % (i.e, 133 m) of the entire Valais. Altogether, these four vegetation classes represent 49.1% of the canton, the rest being mainly bare rocks, water and built-up lands.

Table 1 : Vegetation classes with corresponding area, proportion of the Valais territory and altitude mean.

	Surface (km^2)	*Proportion (%)*	*Altitude mean (m)*
Deciduous trees	484	9.3	1387
Coniferous trees	722	13.8	1558
Grasslands	1176	22.5	2093
Shrubs	133	2.5	2103
Other	2713	51.9	2444

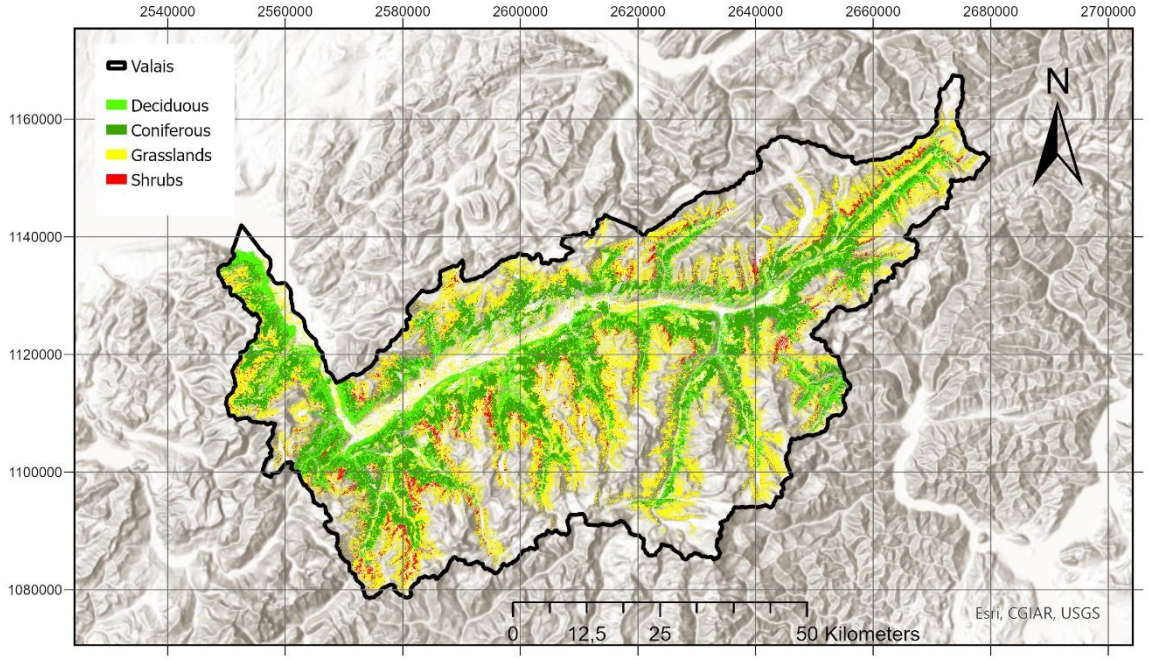

Figure 4 : Vegetation distribution in the Valais (projection : CH1903+ / LV95)

3.2. VIs time series

NDVI

By detailing the NDVI results (figure 5), we note that the raw time series are noisy, particularly in winter/spring and for coniferous trees. For deciduous trees, metrics derived from double logistic function indicate a mean of 0.54 over the entire period and minimum and maximum values of respectively 0.22 and 0.82. In the same ranges, coniferous trees possess a mean of 0.59, with minimum and maximum of 0.23 and 0.8. The mean value for grasslands is lower with 0.34, with minimum and maximum values of 0.06 and 0.56. Comparatively, shrubs depict a slightly higher mean value of 0.40, with 0.04 and 0.77 for minimum and maximum. Regarding the seasonality, we observed a marked cycle for all vegetation classes.

PPI

For the PPI results (figure 6), raw data are also noisy, but in a restrained way, particularly for winter/spring. Regarding metrics derived from double logistic functions, means are equivalent to 0.52, 0.35, 0.43 and 0.41 respectively for deciduous trees, coniferous trees, grasslands and shrubs. Concerning paired minimum and maximum values (min/max), they are of 0.01/1.5 for deciduous trees, 0.06/0.96 for coniferous trees, 0.01/1.13 for grasslands and 0.01/1.54 for shrubs.

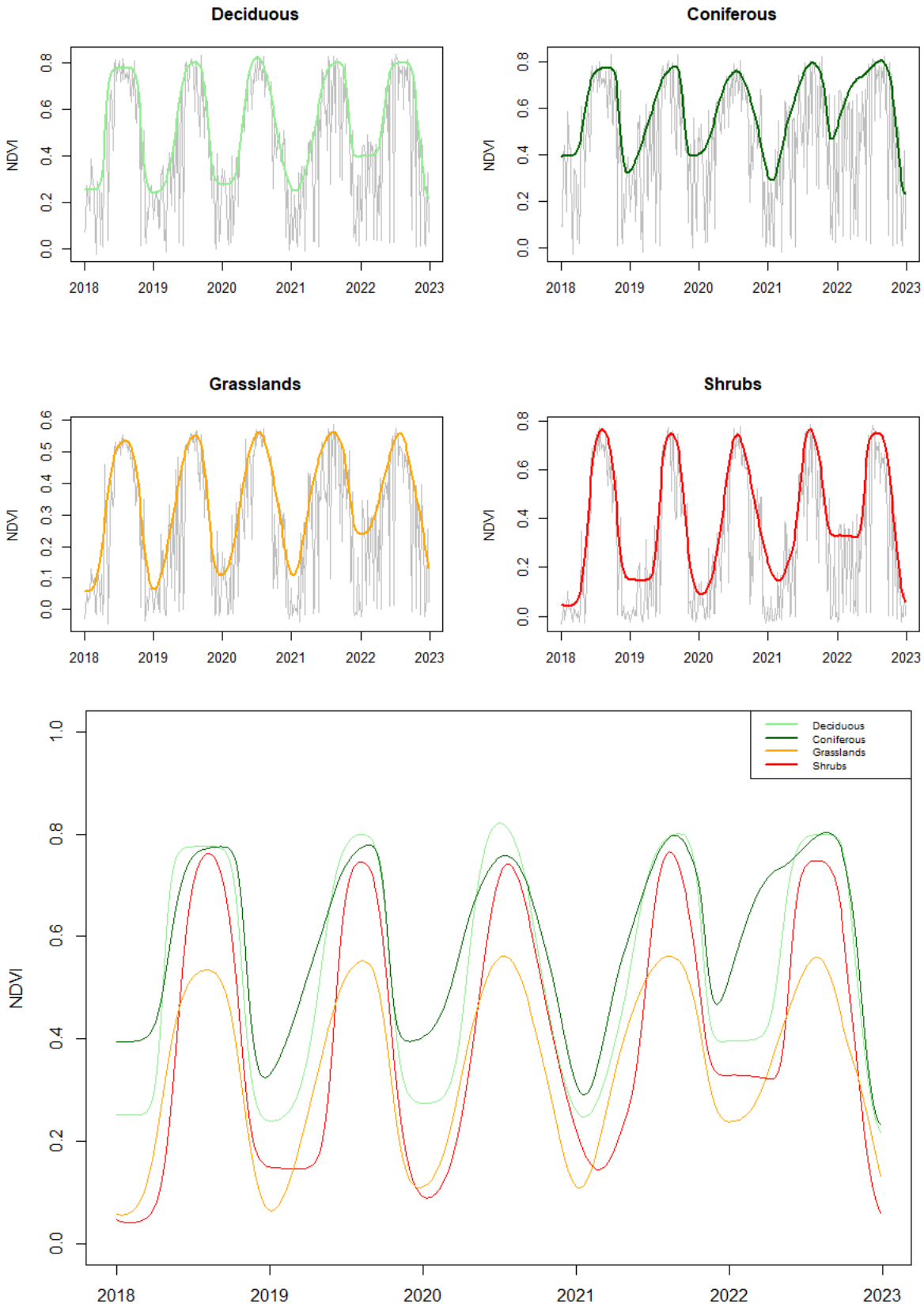

Figure 5 : NDVI time series per vegetations classes (top) with raw data (grey) and the double logistic function derived (colored). The bottom chart depicts all double logistic functions.

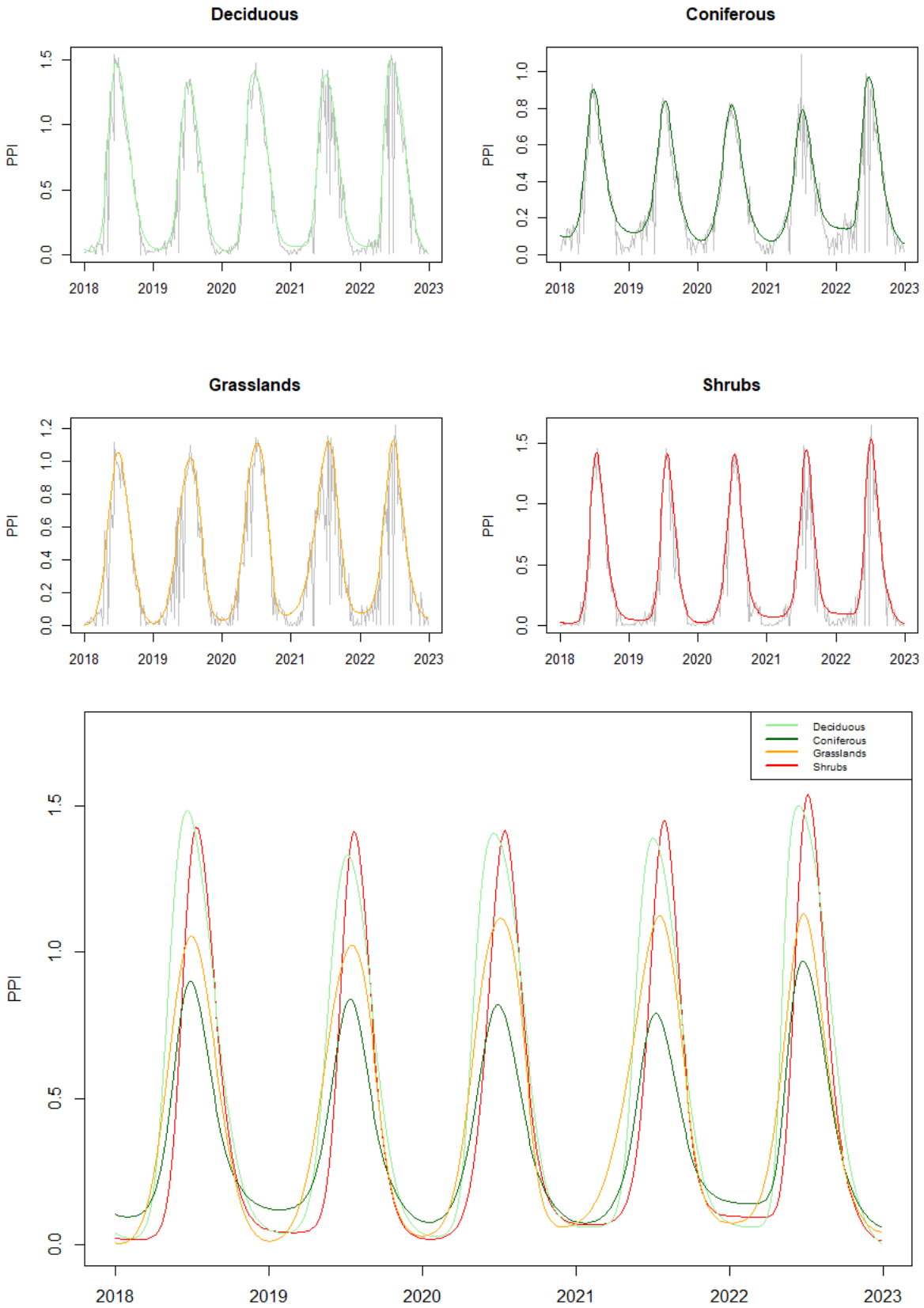

Figure 6 : PPI time series per vegetations classes (top) with raw data (grey) and the double logistic function derived (colored). The bottom chart depicts all double logistic functions.

3.3. Comparison of VIs time series

Regarding VIs time series comparison, we observe that PPI has a higher amplitude than NDVI for all vegetation classes (figure 7). This trend is however less marked for coniferous trees. Additionally, the PPI peaks are more pronounced for deciduous trees, grasslands, and shrubs. We also observe a different annual shape for the two indices, tighter and more elongated for the PPI. The PPI and NDVI indicate different scaled values for coniferous trees. Following a Shapiro test, the time series data are not normally distributed. Therefore, a Spearman correlation test has been executed for each pair of vegetation classes. Resulting Spearman correlation coefficient (rho) are 0.91 for deciduous trees, 0.87 for coniferous trees, 0.93 for grasslands, 0.96 for shrubs with a p-value < 0.05 for each one.

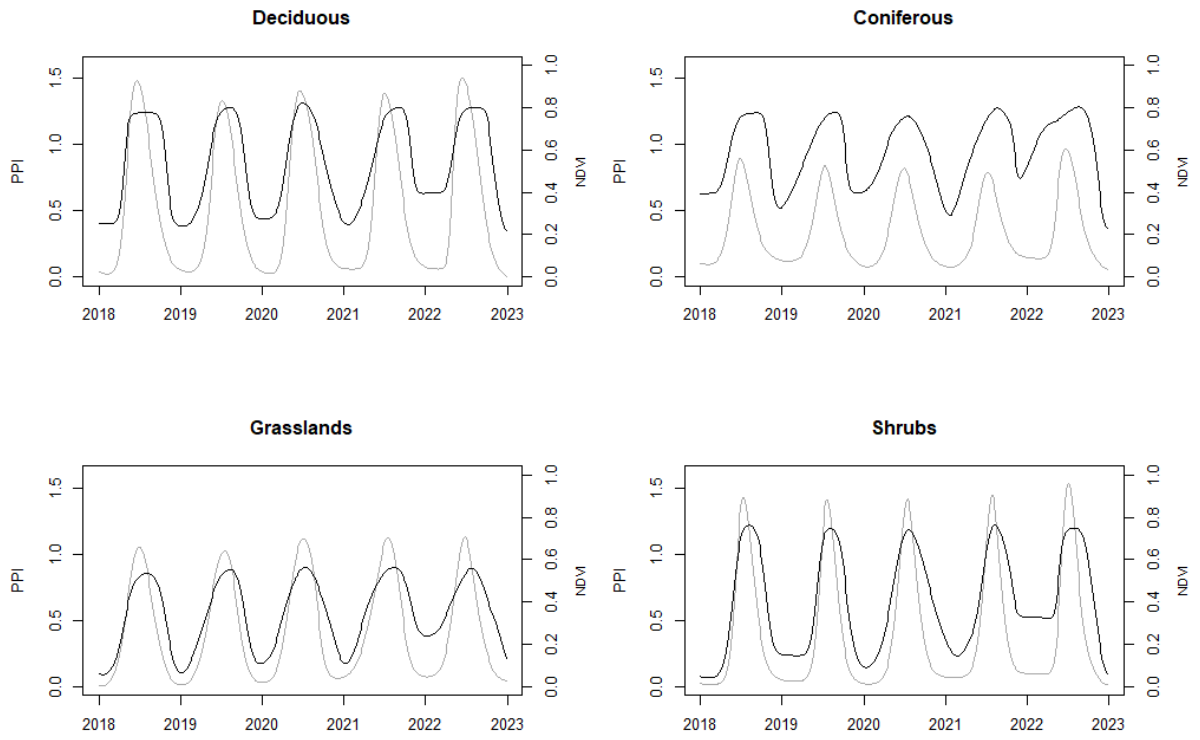

Figure 7 : PPI (grey) and NDVI (black) time series for each vegetation class

3.4. Seasonality parameters retrieval

The seasonality parameters indicate a consistence between the two indices for the retrieval of SOS and EOS for deciduous trees, grasslands and shrubs (table 2). Respectively, the mean differences (PPI-NDVI) for the SOS are 1.4, 1.4 and 4.2 days and for the EOS -1.4, -9.8 and -11.8 days. For coniferous trees, differences are more important and correspond for the SOS to 32.8 days and for the EOS to -12.2 days. According to these differences, the length of the season retrievals diverges less for deciduous trees (-2.8 days), followed by grasslands (-11.2 days), shrubs (-16 days), and coniferous trees (-45 days). For the POS retrieval, the differences are important for all the vegetation classes, with an early detection from PPI.

Table 2 : Seasonality parameters per vegetation types in day of the year (DOY) for PPI and NDVI and in day for differences between PPI and NDVI

		PPI				*NDVI*				*Difference (PPI-NDVI)*			
Deciduous trees	Year	SOS	EOS	Length	POS	SOS	EOS	Length	POS	SOS	EOS	Length	POS
	2018	113	303	190	183	115	310	195	214	-2	-7	-5	-31
	2019	125	309	184	198	118	297	179	218	7	12	5	-20
	2020	110	295	185	184	109	291	182	197	1	4	3	-13
	2021	129	306	177	196	121	308	187	232	8	-2	-10	-36
	2022	120	301	181	181	127	315	188	223	-7	-14	-7	-42
	Mean	***119.4***	***302.8***	***183.4***	***188.4***	***118***	***304.2***	***186.2***	***216.8***	***1.4***	***-1.4***	***-2.8***	***-28.4***
Coniferous trees	2018	121	291	170	188	128	318	190	233	-7	-27	-20	-45
	2019	129	307	178	202	92	292	200	221	37	15	-22	-19
	2020	107	300	193	189	88	317	229	205	19	-17	-36	-16
	2021	124	299	175	198	97	311	214	232	27	-12	-39	-34
	2022	126	299	173	186	38	319	281	216	88	-20	-108	-30
	Mean	***121.4***	***299.2***	***177.8***	***192.6***	***88.6***	***311.4***	***222.8***	***221.4***	***32.8***	***-12.2***	***-45***	***-28.8***
Grasslands	2018	103	303	200	190	111	309	198	217	-8	-6	2	-27
	2019	104	303	199	203	101	297	196	218	3	6	3	-15
	2020	99	285	186	192	91	301	210	200	8	-16	-24	-8
	2021	96	301	205	203	88	307	219	216	8	-6	-14	-13
	2022	108	291	183	184	112	318	206	217	-4	-27	-23	-33
	Mean	***102***	***296.6***	***194.6***	***194.4***	***100.6***	***306.4***	***205.8***	***213.6***	***1.4***	***-9.8***	***-11.2***	***-19.2***
Shrubs	2018	147	294	147	203	144	301	157	226	3	-7	-10	-23
	2019	158	295	137	212	157	299	142	228	1	-4	-5	-16
	2020	138	288	150	204	120	309	189	214	18	-21	-39	-10
	2021	159	291	132	217	158	296	138	230	1	-5	-6	-13
	2022	145	285	140	195	147	307	160	223	-2	-22	-20	-28
	Mean	***149.4***	***290.6***	***141.2***	***206.2***	***145.2***	***302.4***	***157.2***	***224.2***	***4.2***	***- 11.8***	***-16***	***-18***

3.5. PPI and NDVI correlation with GPP in Torgnon (IT)

By retrieving the GPP seasonal dynamics in Torgnon, the correlation with NDVI is higher than with PPI for the 2018 to 2020 years (figure 8). The results of the normality distribution Shapiro test indicate a non-normal distribution for the three datasets. The Spearman correlation coefficients (rho) are equivalent to 0.72 for GPP and PPI and 0.75 for GPP and NDVI ($p < 0.01$). Regarding the data distribution, we note a heteroscedasticity for the PPI facing the GPP. For the NDVI and GPP scatterplot, we note that high NDVI values tend to reach a plateau. The Spearman correlation coefficient between PPI and NDVI is equivalent to 0.9 ($p < 0.01$).

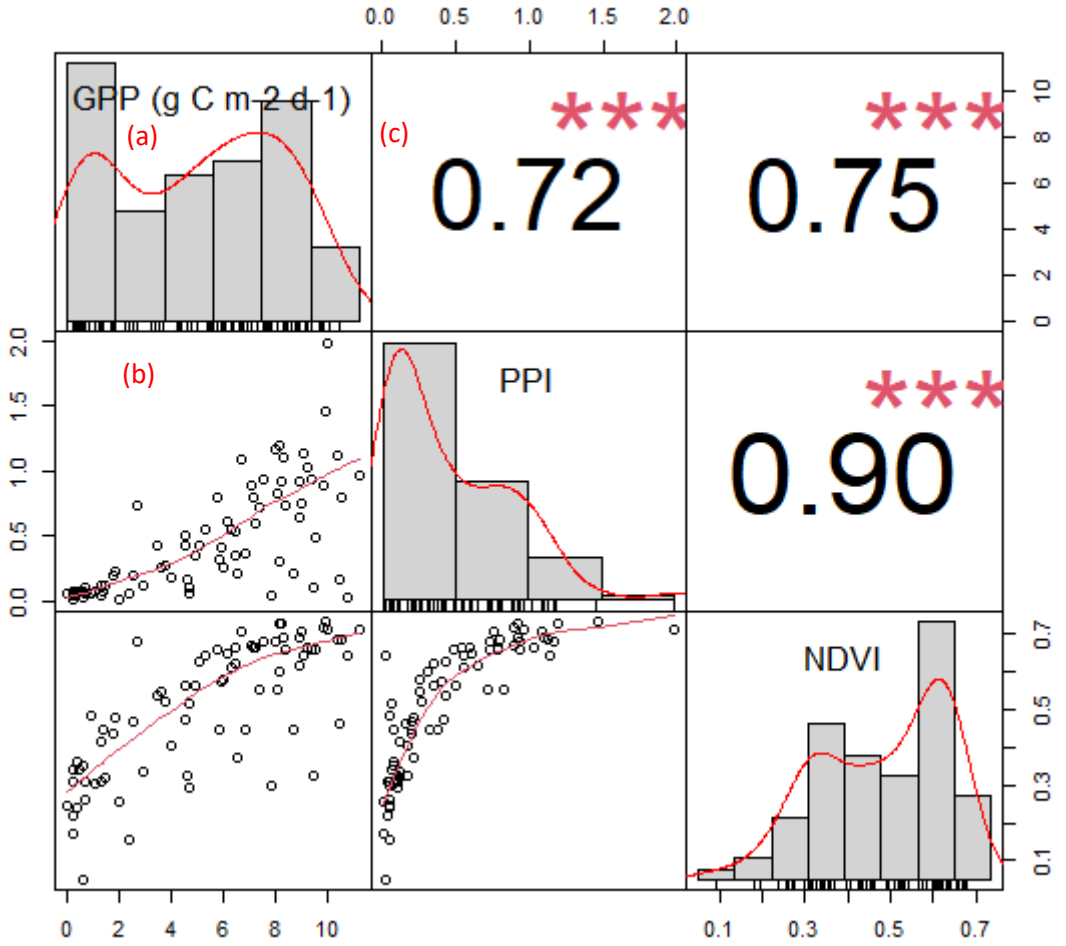

Figure 8 : Correlation chart between GPP, PPI and NDVI with: (a) the distribution of variables of interest by a histogram and a density function; (b) the smoothed regression line between each pair of variables; (c) the Spearman correlation coefficient between each pair of variables ($p < 0.01$)

4. Discussion

4.1. Time series of the PPI and NDVI in mountainous areas for different vegetation types

Our results suggest that the plant phenology index is a robust remote sensed proxy for time series retrieval and phenological monitoring and could be used complementary or as a substitute for NDVI in mountainous areas. NDVI is known as an easy to process remote sensing index but with limitations in snowed environments and for dense vegetation canopy as evergreen forests (Jin & Eklundh, 2014; Jönsson et al., 2010; Tian et al., 2021). The first limit is identifiable with the pronounced noise for winter and beginning/ending of the growing season (figure 5). As mentioned before, the length of the growing season is one of the main determining factors of productivity for vegetation (Leuschner & Ellenberg, 2017) and retrieving the SOS and EOS with precision is therefore of great importance. The snow-sensitivity of NDVI is also characterized by high variation at the beginning and end of the snow season (Jin & Eklundh, 2014). The second limit is also visible with the saturation for coniferous trees at a same level as deciduous trees (approximately 0.8, figure 5 and 7). Tian et al. (2021) found that NDVI struggle in retrieving coniferous trees GPP with a resulting negative correlation for the sites studied.

The PPI seems to deal with these two problems (figure 6). However, accordingly with previous studies (Jin & Eklundh, 2014; Tian et al., 2021), we found that PPI tends to accentuate the signal during the peak growing season (figure 6 and 7), which is induced by its logarithmic formula and therefore its high sensitivity to variability to NIR and red reflectance differences (Tian et al., 2021).

Finally, the different shapes of seasonality curve retrieved by the indices (tighter and longer for the PPI) can be explained by the greater amplitude of the PPI and its tendency to overestimate peaks, coupled with the greater ability of PPI to describe the phenological seasonality of vegetation. It contrast with the NDVI which is more sensitive to snow seasonality, which can influence the accuracy of seasonal parameters retrieval (Jin et al., 2017; Jin & Eklundh, 2014; Tian et al., 2021).

4.2. Seasonality parameters retrieval

By applying different thresholds for seasonality parameters retrieval for PPI and NDVI, we noted a consistency between the two indices for SOS, EOS and length of the season retrieval for deciduous trees, grasslands and shrubs (table 2). However, this is not the case for the POS and for all coniferous trees parameters.

Regarding SOS and EOS retrieval, we based our methodology on amplitude thresholds, identified by Tian et al. (2021), showing the best correspondence between PPI and NDVI and ground-observed phenological stages. This method gave us close results between the two indices (except for conifers). However, to go further in the phenological signification of these indices thresholds, Jin et al. (2017) demonstrated in a precedent study which aimed to disentangle remotely measured plant phenology and snow seasonality that NDVI-derived land surface phenology aligns better with snow seasonality than with actual plant phenology, in contrast to the PPI which is well aligned with ground phenology observation and GPP dynamics. They explained that by the existing linearity between PPI and LAI. As defended by Tian et al. (2021), performances of VIs are not only determined by vegetation changes identification but also by their robustness against background noise. Overall, the use of PPI demonstrates better performance for SOS and EOS retrieving in areas with seasonal snow cover and should therefore be considered (Jin et al., 2017; Karkauskaite et al., 2017; Tian et al., 2021).

Regarding the differences for POS identification, we could legitimately expect that the PPI's tendency to overemphasize seasonal peaks (see 5.1.) have an influence. To solve this issue, Tian et al. (2021) mention the possibility to apply an outlier filter. For coniferous trees, the high noisy signal and the plateau of the NDVI (figure 5 and 7) are likely due to its known problems in retrieving the signal for this class of vegetation (see 5.1.) and influence therefore all seasonality parameters retrieval (Karkauskaite et al., 2017). Therefore, the PPI seems also more reliable for dense coniferous forest.

4.3. Correlation of PPI and NDVI with ground GPP data

Interestingly and to feed the discussion, the NDVI perform a little better in retrieving GPP signal in Torgnon (figure 8). The resulting correlation coefficients are high for both indices (respectively 0.72 and 0.75 for PPI and NDVI) and are consistent with the existing literature (Tian et al., 2021). It is however important to remember that the specific site of Torgnon is a grassland located at 2106 m. It would be necessary to repeat the process over more grasslands but also other vegetation types in the Alps to assess a representative trend. Indeed, by assessing the performance of VIs over 49 GPP sites across Europe, Tian et al. (2021) demonstrate that PPI shows the best consistency in tracking GPP seasonal dynamics and have the lowest variation between different vegetation cover. As mentioned before, NDVI-derived phenology tends to be more related with snow seasonality, in contrast to PPI and its almost linear relationship with LAI (Jin et al., 2017; Tian et al., 2021). Further calibration samples over the Alps are therefore needed.

4.4. Study limitations

The accuracy of the study could be improved by using Level-2A Sentinel-2 images (i.e., surface reflectance) instead of Level 1-C (top of atmosphere). To do so, we recommend to use the Sen2cor program (Main-Knorn et al., 2017) to correct the atmospheric effects from Level-1C images. The pre-processing of high volume of images used for this study (n = 2920, > 600 Go) was challenging in terms of computation time and power. To conduct further studies, such as pixel-scaled spatial analysis, high-performance computing should be considered. Recent developments of data cubes to produce and distribute analysis ready data is also a promising way to reduce the time of pre-processing, which frees up time and capacity for more in-depth studies. Our vegetation mapping method doesn't permit to identify evergreen non-*Ericaceae* shrubs which results in incomplete determination of this class of vegetation and its dynamics. More ground data (i.e., GPP and phenological stages) would be needed for mountainous areas and ideally for Valais to better assess the performance of the indices in seasonal cycle and seasonal parameters retrieval. Furthermore, our study focuses on the behaviour of four main classes of vegetation over the entire Valais region. It would be interesting to (i) include more detailed vegetation types and (ii) to assess spatial trends at pixel resolution.

4.5. Contributions and perspectives

Jin & Eklundh (2014) developed the PPI primarily to improve monitoring of evergreen coniferous forest phenology at high northern latitude. However, they noted that PPI is a robust vegetation index for tracking vegetation phenology and should therefore be tested across more ranges of conditions. This has been done notably for GPP estimation productivity in African semi-arid ecosystems (Abdi et al., 2019) and by the calibration of the Copernicus Europe-wide phenology dataset (Tian et al., 2021). However, to our knowledge, no study has been done specifically for the application of PPI in mountainous areas and more specifically in European Alps (e.g., Valais), where NDVI remains the most used remote sensing index for vegetation phenology and productivity monitoring. Therefore, the main contribution of this study is to assess the potential of PPI in alpine areas, characterized notably by seasonal snow cover and the presence of coniferous forest. The results are promising, the PPI provide a solid remote sensed opportunity for both phenological and productivity monitoring. Furthermore, our study supports that the recently launched Sentinel-2 satellites constellation offers great possibilities for more accurate studies with its 10 m resolution and 5-days revisit time, notably for complex environments as mountainous areas. To go further we suggest (i) to run more comparisons with specific ground data for the Alps and (ii) to execute pixel-resolution analysis for future studies.

Conclusion

In this study we compared and assessed the performance of the Plant Phenology Index (PPI) and Normalized Difference Vegetation Index (NDVI) in mountainous areas, more specifically in the European Alps. We extracted NDVI and PPI values derived from MultiSpectral Instrument on board the Sentinel-2 satellites constellation for the 2018 to 2022 years. Regarding seasonal cycle, the NDVI retrieves a particularly noisy signal around the snowed season (late autumn to early spring) and for coniferous trees. The PPI is less noisy in the early and late season, which could be explained by its low sensibility to snow, its almost linear relationship with LAI and its ability to retrieve effective plant phenology. However, the PPI tends to overestimate the peak of the season, which could be explained by its logarithmic formula and therefore its high sensitivity to NIR and red reflectance difference variations. Concerning the seasonal parameters retrieving, we observe consistency between the two indices with only small differences for the start and end of the season for deciduous trees, grasslands, and shrubs. However, we note important differences for the estimation of the peak of the season and for all the seasonal parameters of coniferous trees. When analyzing the correlation with ground-

measured GPP in an alpine grassland in Torgnon (IT), the Spearman correlation coefficient is more important for NDVI (0.75) but is also high for PPI (0.72).

Our results are consistent with existing literature. It provides new insights for vegetation monitoring in complex environments. However, the accuracy of our study could be enhanced by using L2A Sentinel-2 images, by a more detailed vegetation mapping (e.g., non-*Ericaceae* shrubs) and especially by the use of more ground data to assess in greater detail the performance of indices on different types of vegetation in the Alps. By using high performance computing, it would be also interesting to retrieve spatial trends at pixel resolution.

The main contribution of this study is to assess the performance of PPI in mountainous areas in the European Alps. This index provides a solid approach to monitor vegetation dynamics, in these areas characterized by the presence of seasonal snow and coniferous forest and can be used to overcome NDVI limitations.

References

Abdi, A. M., Boke-Olén, N., Jin, H., Eklundh, L., Tagesson, T., Lehsten, V., & Ardö, J. (2019). First assessment of the plant phenology index (PPI) for estimating gross primary productivity in African semi-arid ecosystems. *International Journal of Applied Earth Observation and Geoinformation*, *78*, 249–260. https://doi.org/10.1016/j.jag.2019.01.018

Asam, S., Callegari, M., Matiu, M., Fiore, G., De Gregorio, L., Jacob, A., Menzel, A., Zebisch, M., & Notarnicola, C. (2018). Relationship between Spatiotemporal Variations of Climate, Snow Cover and Plant Phenology over the Alps—An Earth Observation-Based Analysis. *Remote Sensing*, *10*(11), Article 11. https://doi.org/10.3390/rs10111757

Baldocchi, D., Falge, E., Gu, L., Olson, R., Hollinger, D., Running, S., Anthoni, P., Bernhofer, C., Davis, K., Evans, R., Fuentes, J., Goldstein, A., Katul, G., Law, B., Lee, X., Malhi, Y., Meyers, T., Munger, W., Oechel, W., … Wofsy, S. (2001). FLUXNET: A New Tool to Study the Temporal and Spatial Variability of Ecosystem–Scale Carbon Dioxide, Water Vapor, and Energy Flux Densities. *Bulletin of the American Meteorological Society*, *82*(11), 2415–2434. https://doi.org/10.1175/1520-0477(2001)082<2415:FANTTS>2.3.CO;2

Baumann, P. (2017). *The Datacube Manifesto*. https://earthserver.eu/tech/datacube-manifesto/

Bayle, A., Carlson, B. Z., Nicoud, B., Francon, L., Corona, C., & Choler, P. (in press). *Biogeographical distribution and limiting factors of Ericaceae- dominated shrublands in the French Alps: Towards improved understanding of alpine shrubification*.

Bayle, A., Carlson, B. Z., Thierion, V., Isenmann, M., & Choler, P. (2019). Improved Mapping of Mountain Shrublands Using the Sentinel-2 Red-Edge Band. *Remote Sensing*, *11*(23), Article 23. https://doi.org/10.3390/rs11232807

Beniston, M., Farinotti, D., Stoffel, M., Andreassen, L. M., Coppola, E., Eckert, N., Fantini, A., Giacona, F., Hauck, C., Huss, M., Huwald, H., Lehning, M., López-Moreno, J.-I., Magnusson, J., Marty, C., Morán-Tejéda, E., Morin, S., Naaim, M., Provenzale, A., … Vincent, C. (2018). The European mountain cryosphere: A review of its current state, trends, and future challenges. *The Cryosphere*, *12*(2), 759–794. https://doi.org/10.5194/tc-12-759-2018

Berner, L. T., Massey, R., Jantz, P., Forbes, B. C., Macias-Fauria, M., Myers-Smith, I., Kumpula, T., Gauthier, G., Andreu-Hayles, L., Gaglioti, B. V., Burns, P., Zetterberg, P., D'Arrigo, R., & Goetz, S. J. (2020). Summer warming explains widespread but not uniform greening in the Arctic tundra biome. *Nature Communications*, *11*(1), Article 1. https://doi.org/10.1038/s41467-020-18479-5

Carlson, B. Z. (2016). *Understanding spatial patterns of diversity and productivity in alpine plant communities: Application of high-resolution imagery in the French Alps*.

Carlson, B. Z., Corona, M. C., Dentant, C., Bonet, R., Thuiller, W., & Choler, P. (2017). Observed long-term greening of alpine vegetation—A case study in the French Alps. *Environmental Research Letters*, *12*(11), 114006. https://doi.org/10.1088/1748-9326/aa84bd

Choler, P. (2015). Growth response of temperate mountain grasslands to inter-annual variations in snow cover duration. *Biogeosciences*, *12*(12), 3885–3897. https://doi.org/10.5194/bg-12-3885-2015

Choler, P., Bayle, A., Carlson, B. Z., Randin, C., Filippa, G., & Cremonese, E. (2021). The tempo of greening in the European Alps: Spatial variations on a common theme. *Global Change Biology*, *27*(21), 5614–5628. https://doi.org/10.1111/gcb.15820

Corona-Lozada, M. C., Morin, S., & Choler, P. (2019). Drought offsets the positive effect of summer heat waves on the canopy greenness of mountain grasslands. *Agricultural and Forest Meteorology*, *276–277*, 107617. https://doi.org/10.1016/j.agrformet.2019.107617

Eklund, L., & Jönsson, P. (2017). *Timesat 3.3 Software Manual*. Lund and Malmö University, Sweden.

European Environment Agency. (2020a). *Forest Type 2018 (raster 10 m), Europe, 3-yearly, Oct. 2020* (01.00) [GeoTIFF]. European Environment Agency. https://doi.org/10.2909/59B0620C-7BB4-4C82-B3CE-F16715573137

European Environment Agency. (2020b). *Grassland 2018 (raster 10 m), Europe, 3-yearly, Aug. 2020* (01.00) [GeoTIFF]. European Environment Agency. https://doi.org/10.2909/60639D5B-9164-4135-AE93-FB4132BB6D83

European Environment Agency. (2021b). *High Resolution Vegetation Phenology and Productivity: Normalized Difference Vegetation Index (raster 10m) - version 1 revision 1, Sep. 2021* (01.01) [GeoTIFF]. European Environment Agency. https://doi.org/10.2909/5D5F72CE-80BC-4C90-80ED-F135596533E2

European Environment Agency. (2021a). *High Resolution Vegetation Phenology and Productivity: Plant Phenology Index (raster 10m) version 1 revision 1, Sep. 2021* (01.01) [GeoTIFF]. European Environment Agency. https://doi.org/10.2909/65F095AF-5225-490B-8A29-4500D4C31B8A

Filippa, G., Cremonese, E., Galvagno, M., Bayle, A., Choler, P., Bassignana, M., Piccot, A., Poggio, L., Oddi, L., Gascoin, S., Costafreda-Aumedes, S., Argenti, G., & Dibari, C. (2022). On the distribution and productivity of mountain grasslands in the Gran Paradiso National Park, NW Italy: A remote sensing approach. *International Journal of Applied Earth Observation and Geoinformation*, *108*, 102718. https://doi.org/10.1016/j.jag.2022.102718

Filippa, G., Cremonese, E., Galvagno, M., Isabellon, M., Bayle, A., Choler, P., Carlson, B. Z., Gabellani, S., Morra di Cella, U., & Migliavacca, M. (2019). Climatic Drivers of Greening Trends in the Alps. *Remote Sensing*, *11*(21), 2527. https://doi.org/10.3390/rs11212527

Francon, L., Corona, C., Roussel, E., Lopez Saez, J., & Stoffel, M. (2017). Warm summers and moderate winter precipitation boost Rhododendron ferrugineum L. growth in the Taillefer massif (French Alps). *Science of The Total Environment*, *586*, 1020–1031. https://doi.org/10.1016/j.scitotenv.2017.02.083

Francon, L., Corona, C., Till-Bottraud, I., Choler, P., Carlson, B. Z., Charrier, G., Améglio, T., Morin, S., Eckert, N., Roussel, E., Lopez-Saez, J., & Stoffel, M. (2020). Assessing the effects of earlier snow melt-out on alpine shrub growth: The sooner the better? *Ecological Indicators*, *115*, 106455. https://doi.org/10.1016/j.ecolind.2020.106455

Giuliani, G., Chatenoux, B., De Bono, A., Rodila, D., Richard, J.-P., Allenbach, K., Dao, H., & Peduzzi, P. (2017). Building an Earth Observations Data Cube: Lessons learned from the Swiss Data Cube

(SDC) on generating Analysis Ready Data (ARD). *Big Earth Data*, *1*(1–2), 100–117. https://doi.org/10.1080/20964471.2017.1398903

Giuliani, G., Rodila, D., Külling, N., Maggini, R., & Lehmann, A. (2022). Downscaling Switzerland Land Use/Land Cover Data Using Nearest Neighbors and an Expert System. *Land*, *11*(5), 615. https://doi.org/10.3390/land11050615

Gobiet, A., Kotlarski, S., Beniston, M., Heinrich, G., Rajczak, J., & Stoffel, M. (2014). 21st century climate change in the European Alps—A review. *Science of The Total Environment*, *493*, 1138–1151. https://doi.org/10.1016/j.scitotenv.2013.07.050

Gorelick, N., Hancher, M., Dixon, M., Ilyushchenko, S., Thau, D., & Moore, R. (2017). Google Earth Engine: Planetary-scale geospatial analysis for everyone. *Remote Sensing of Environment*, *202*, 18–27. https://doi.org/10.1016/j.rse.2017.06.031

Hijmans R (2023a). _terra: Spatial Data Analysis_. R package version 1.7-3, <https://CRAN.R-project.org/package=terra>.

Hijmans R (2023b). _raster: Geographic Data Analysis and Modeling_. R package version 3.6-14, <https://CRAN.R-project.org/package=raster>.

IPCC. (2021). Annex X: Expert Reviewers of the IPCC Working Group I Sixth Assessment Report. In V. Masson-Delmotte, P. Zhai, A. Pirani, S. L. Connors, C. Péan, S. Berger, N. Caud, Y. Chen, L. Goldfarb, M. I. Gomis, M. Huang, K. Leitzell, E. Lonnoy, J. B. R. Matthews, T. K. Maycock, T. Waterfield, O. Yelekçi, R. Yu, & B. Zhou (Eds.), *Climate Change 2021: The Physical Science Basis. Contribution of Working Group I to the Sixth Assessment Report of the Intergovernmental Panel on Climate Change* (pp. 2287–2338). Cambridge University Press.

Jin, H., & Eklundh, L. (2014). A physically based vegetation index for improved monitoring of plant phenology. *Remote Sensing of Environment*, *152*, 512–525. https://doi.org/10.1016/j.rse.2014.07.010

Jin, H., Jönsson, A. M., Bolmgren, K., Langvall, O., & Eklundh, L. (2017). Disentangling remotely-sensed plant phenology and snow seasonality at northern Europe using MODIS and the plant phenology index. *Remote Sensing of Environment*, *198*, 203–212. https://doi.org/10.1016/j.rse.2017.06.015

Jin, H., Jönsson, A. M., Olsson, C., Lindström, J., Jönsson, P., & Eklundh, L. (2019). New satellite-based estimates show significant trends in spring phenology and complex sensitivities to temperature and precipitation at northern European latitudes. *International Journal of Biometeorology*, *63*(6), 763–775. https://doi.org/10.1007/s00484-019-01690-5

Jönsson, A. M., Eklundh, L., Hellström, M., Bärring, L., & Jönsson, P. (2010). Annual changes in MODIS vegetation indices of Swedish coniferous forests in relation to snow dynamics and tree phenology. *Remote Sensing of Environment*, *114*(11), 2719–2730. https://doi.org/10.1016/j.rse.2010.06.005

Jönsson, P., & Eklundh, L. (2002). Seasonality extraction by function fitting to time-series of satellite sensor data. *IEEE Transactions on Geoscience and Remote Sensing*, *40*(8), 1824–1832. https://doi.org/10.1109/TGRS.2002.802519

Jönsson, P., & Eklundh, L. (2004). TIMESAT—a program for analyzing time-series of satellite sensor data. *Computers & Geosciences*, *30*(8), 833–845. https://doi.org/10.1016/j.cageo.2004.05.006

Karkauskaite, P., Tagesson, T., & Fensholt, R. (2017). Evaluation of the Plant Phenology Index (PPI), NDVI and EVI for Start-of-Season Trend Analysis of the Northern Hemisphere Boreal Zone. *Remote Sensing*, *9*(5), Article 5. https://doi.org/10.3390/rs9050485

Keenan, T. F., & Riley, W. J. (2018). Greening of the land surface in the world's cold regions consistent with recent warming. *Nature Climate Change*, *8*(9), Article 9. https://doi.org/10.1038/s41558-018-0258-y

Körner, C. (2021). *Alpine Plant Life: Functional Plant Ecology of High Mountain Ecosystems* (Third Edition). Springer International Publishing. https://doi.org/10.1007/978-3-030-59538-8

Kuenzer, C., Dech, S., & Wagner, W. (Eds.). (2015). *Remote Sensing Time Series: Revealing Land Surface Dynamics* (Vol. 22). Springer International Publishing. https://doi.org/10.1007/978-3-319-15967-6

Leuschner, C., & Ellenberg, H. (2017). Vegetation of the Alpine and Nival Belts. In C. Leuschner & H. Ellenberg (Eds.), *Ecology of Central European Non-Forest Vegetation: Coastal to Alpine, Natural to Man-Made Habitats: Vegetation Ecology of Central Europe, Volume II* (pp. 271–431). Springer International Publishing. https://doi.org/10.1007/978-3-319-43048-5_5

Main-Knorn, M., Pflug, B., Louis, J., Debaecker, V., Müller-Wilm, U., & Gascon, F. (2017). Sen2Cor for Sentinel-2. In L. Bruzzone, F. Bovolo, & J. A. Benediktsson (Eds.), *Image and Signal Processing for Remote Sensing XXIII* (p. 3). SPIE. https://doi.org/10.1117/12.2278218

Myers-Smith, I. H., Kerby, J. T., Phoenix, G. K., Bjerke, J. W., Epstein, H. E., Assmann, J. J., John, C., Andreu-Hayles, L., Angers-Blondin, S., Beck, P. S. A., Berner, L. T., Bhatt, U. S., Bjorkman, A. D., Blok, D., Bryn, A., Christiansen, C. T., Cornelissen, J. H. C., Cunliffe, A. M., Elmendorf, S. C., … Wipf, S. (2020). Complexity revealed in the greening of the Arctic. *Nature Climate Change*, *10*(2), 106–117. https://doi.org/10.1038/s41558-019-0688-1

Papale, D. (2020). Ideas and perspectives: Enhancing the impact of the FLUXNET network of eddy covariance sites. *Biogeosciences*, *17*(22), 5587–5598. https://doi.org/10.5194/bg-17-5587-2020

Pastorello, G., Trotta, C., Canfora, E. *et al.* The FLUXNET2015 dataset and the ONEFlux processing pipeline for eddy covariance data. *Sci Data* **7**, 225 (2020). https://doi.org/10.1038/s41597-020-0534-3

Peterson BG, Carl P (2020). _PerformanceAnalytics: Econometric Tools for Performance and Risk Analysis_. R package version 2.0.4, <https://CRAN.R-project.org/package=PerformanceAnalytics>.

Poussin, C., Massot, A., Ginzler, C., Weber, D., Chatenoux, B., Lacroix, P., Piller, T., Nguyen, L., & Giuliani, G. (2021). Drying conditions in Switzerland – indication from a 35-year Landsat time-series analysis of vegetation water content estimates to support SDGs. *Big Earth Data*, *5*(4), 445–475. https://doi.org/10.1080/20964471.2021.1974681

R Core Team (2023). R: A language and environment for statistical computing. R Foundation for Statistical Computing, Vienna, Austria. URL https://www.R-project.org/

Smets, B., Zhanzhang, C., Eklundh, L., Tian, F., Bonte, K., Van Hoost, R., Van De Kerchove, R., Adriaensen, S., De Roo, B., Jacobs, T., Camacho, F., Sánchez-Zapero, J., Swinnen, E., Scheifinger, H., Hufkens, K., & Jönsson, P. (2022). *Copernicus Land Monitoring Service HIGH RESOLUTION VEGETATION PHENOLOGY AND PRODUCTIVITY (HR-VPP), Daily Raw Vegetation Indices* (p. 39). European Environment Agency (EEA). https://land.copernicus.eu/user-corner/technical-library/product-user-manual-of-vegetation-indices

Stanimirova, Cai, Melaas, Gray, Eklundh, Jönsson, & Friedl. (2019). An Empirical Assessment of the MODIS Land Cover Dynamics and TIMESAT Land Surface Phenology Algorithms. *Remote Sensing*, *11*(19), 2201. https://doi.org/10.3390/rs11192201

Tang, J., Körner, C., Muraoka, H., Piao, S., Shen, M., Thackeray, S. J., & Yang, X. (2016). Emerging opportunities and challenges in phenology: A review. *Ecosphere*, *7*(8), e01436. https://doi.org/10.1002/ecs2.1436

Tian, F., Cai, Z., Jin, H., Hufkens, K., Scheifinger, H., Tagesson, T., Smets, B., Van Hoolst, R., Bonte, K., Ivits, E., Tong, X., Ardö, J., & Eklundh, L. (2021). Calibrating vegetation phenology from Sentinel-2 using eddy covariance, PhenoCam, and PEP725 networks across Europe. *Remote Sensing of Environment*, *260*, 112456. https://doi.org/10.1016/j.rse.2021.112456

Tucker, C. J. (1979). Red and photographic infrared linear combinations for monitoring vegetation. *Remote Sensing of Environment*, *8*(2), 127–150. https://doi.org/10.1016/0034-4257(79)90013-0

Vorkauf, M., Kahmen, A., Körner, C., & Hiltbrunner, E. (2021). Flowering phenology in alpine grassland strongly responds to shifts in snowmelt but weakly to summer drought. *Alpine Botany*, *131*(1), 73–88. https://doi.org/10.1007/s00035-021-00252-z

Wipf, S., Stoeckli, V., & Bebi, P. (2009). Winter climate change in alpine tundra: Plant responses to changes in snow depth and snowmelt timing. *Climatic Change*, *94*(1–2), 105–121. https://doi.org/10.1007/s10584-009-9546-x

Xie, Y., Sha, Z., & Yu, M. (2008). Remote sensing imagery in vegetation mapping: A review. *Journal of Plant Ecology*, *1*(1), 9–23. https://doi.org/10.1093/jpe/rtm005